Essential Readings in Light Metals: Electrode Technology for Aluminum Production.
Edited by Alan Tomsett and John Johnson.

PROBLEMS OF THE STUB – ANODE CONNECTION

Siegfried Wilkening[1], Jules Côté[2]
[1] TC Carbon & Graphite / Aluminium Smelting, Mühlenstr. 16, 53347 Alfter, Germany
[2] Aluminerie Alouette Inc., Case Postal 1650, Sept Iles, Quebec, Canada G4R5M9

Keywords: Stub Contact, Anode Voltage Drop, Contact Voltage

Abstract

The voltage drop between stub and anode is an essential part of the overall voltage drop in the anode section and has an impact on the electrolytic process. Relevant physical properties of stub steel, cast iron and anode carbon have been measured in this context. Results of various voltage drop measurements between stub and anode in industrial cells as well as in laboratory devices are presented and discussed. It is mainly the contact pressure by which millivolts are gained between cast-iron sealed stubs and carbon anodes.

Introduction

The main steps of voltage drop in the anode section of an aluminium reduction cell are outlined in Figure 1. The Ohmic heat, which is generated below the vault of crust and insulating layer of anode cover material, has a strong thermal effect on the electrolytic bath, and should be minimized. The less heat is evolved in the anode section, the more heat can be generated in the electrolyte. This allows an increase in anode-cathode distance (ACD), which in turn is favorable when aiming at boosting of current density, current efficiency and improvement of MHD stability. As practical measurements have shown, the stub-anode voltage drop is of the same order of magnitude as the average voltage drop in the anode block during its cycle or rota time. It is believed that the potential in reducing the voltage drop between stub and anode is greater than in the anode itself.

Principally, the cast-iron connection between stub and anode, as depicted in Figure 2, performs in practice over a wide range of contact conditions and respective voltage drops from bad to good.

In a conventional design (see Figure 2), a cylindrical stub is inserted into a conical stubhole, i.e. the cast-iron thimble has a lower wall thickness at the tip of the stub than in the upper part of the stubhole. It is a basic drawback of cast-iron rodding that the contact between the unit stub & thimble and the stubhole wall is loose at ambient temperatures and becomes tight with rising temperatures. Depending on the cast-iron composition and the casting conditions, the shrinkage of cast iron in the upper, thick-wall part is usually higher than in the lower, thin-wall part of the thimble. As a consequence, the contact pressure will first rise near the bottom end of the stub and is additionally increased by the higher temperatures at this place. Therefore, a less inclined taper of the stubhole seems to be advantageous. Almost no current is transferred through the circular bottom of the stub because of missing contact pressure. Figure 3 shows the course of a typical stub-anode voltage drop as a function of time and temperature. If the design and casting conditions are optimal, the voltage drop decreases continuously and levels off at about 500°C.

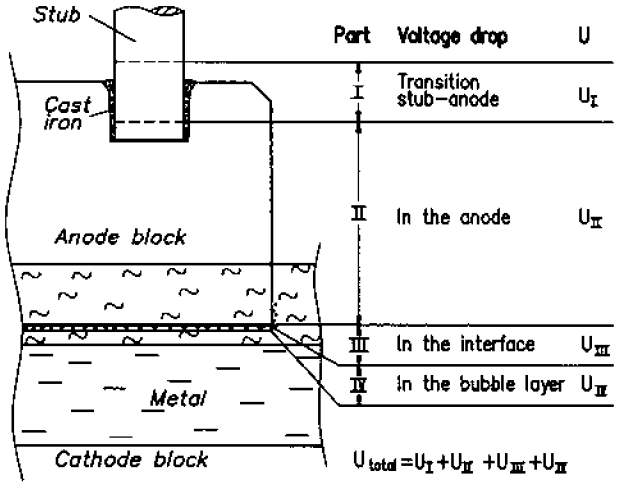

Figure 1:Steps of voltage drop in the anode section

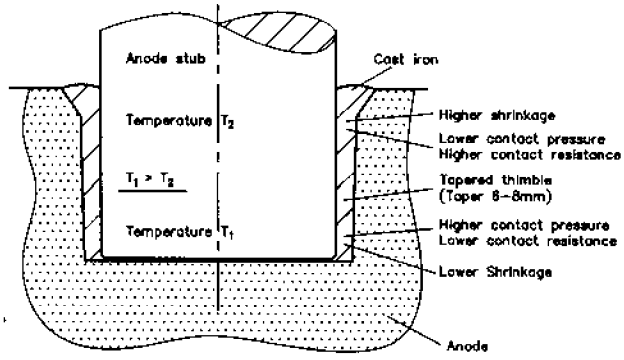

Figure 2: Ordinary design of the stub – anode connection

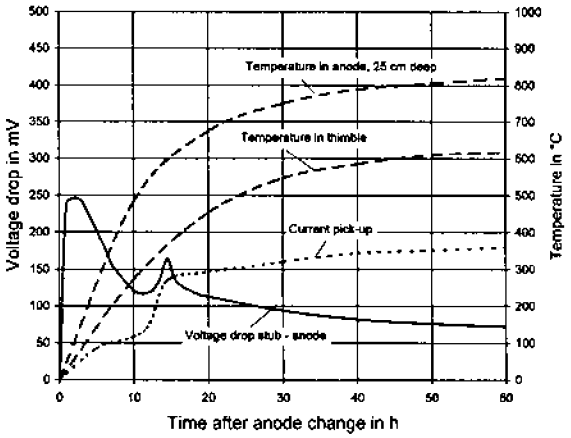

Figure 3: Typical voltage drop between stub / thimble and anode after anode change

Material Properties

This paper focuses on the presently applied stub-anode connection of prebaked anodes. It consists of the three consecutively arranged materials steel, cast iron and anode carbon. In the early days of aluminium electrolysis a direct contact between the steel pin and anode was used. The conical steel pin had a sharp-edged conical thread and was screwed into a slightly tapered stubhole of the prebaked anode block. In reduction cells with Søderberg anodes there is still the direct contact between steel studs and coked Søderberg paste. Other types of stub-anode connections are known where the electrically conductive bridge between steel stub and anode was made by ramming or gluing pastes.

The main physical properties, which play a role in the stub-anode connection, are thermal expansion, electrical resistivity and thermal conductivity.

Thermal expansion

Typical thermal expansion curves of steel, cast iron and anode carbon are shown in Figures 4 to 9. It can be taken as a rule of thumb that the thermal expansion of steel is about three times higher than that of anode carbon. The $\alpha - \gamma$ phase transition in the thermal expansion of steel and cast iron has a measurable effect on the contact pressure and voltage drop.

Rapidly cooled cast iron contains the carbon in form of iron carbide, Fe_3C, or cementite. At annealing temperatures above 700°C, cementite is decomposed and free graphite is precipitated in the iron structure. This precipitation of graphite causes a permanent volume expansion, as can be seen from the cooling curve of cast iron or from a second run of thermal expansion measurement. The graphite precipitation adds to the contact pressure and thus to a lower voltage drop. For this reason, a high carbon content of cast iron above 3.4% is advantageous.

The thermal expansion of the carbon anode is different in the vertical and horizontal direction, i.e. perpendicular or parallel to the forming plane. When considering the stub-anode contact pressure, the lower expansion values in the horizontal direction have to be applied.

Electrical resistivity

The electrical resistivity of steel (see Figure 10) increases almost by a factor of ten between room temperature and 1000°C. In the temperature range of the α-γ transition its resistivity rests at a level because of the higher density of γ-iron. The electrical resistivity of cast iron (see Figures 12 and 13) is substantially higher than that of steel but it does not increase with temperature at the same rate as steel. The electrical resistance of the cast iron thimble decreases with heat treatment or with intrinsic precipitation of graphite, and is of minor importance, because it is crossed by the current only over a short distance.

The lower electrical resistivity of the carbon anode in the horizontal direction (see Figure 9) counts with respect to the cylindrical contact area with cast iron. It is a significant aspect that the electrical resistance of anode carbon decreases with temperature and also with higher apparent density (see Figure 10) because the current density in the anode carbon is comparatively high at the interface with cast iron.

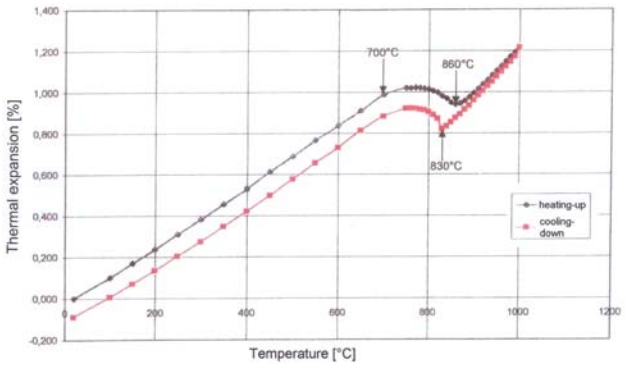

Figure 4: Thermal expansion of new mild steel

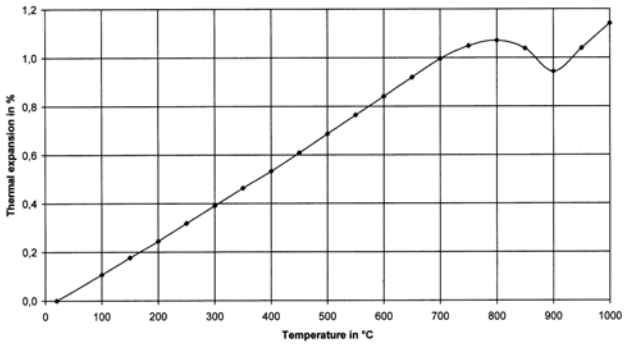

Figure 5: Expansion of Alouette stub steel S

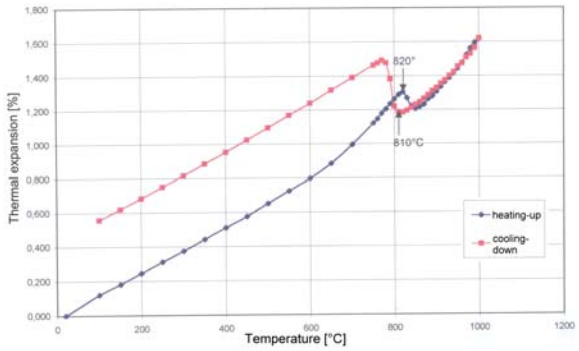

Figure 6: Thermal expansion of cast iron, first heating-up

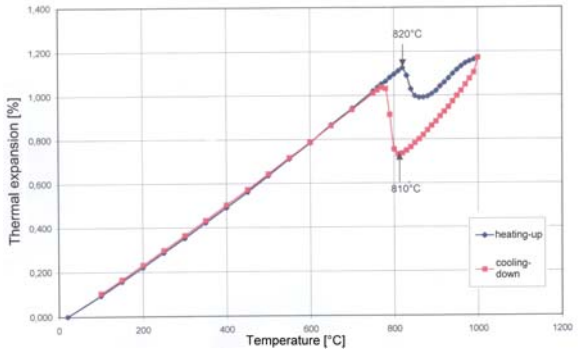

Figure 7: Thermal expansion of cast iron, second heating-up

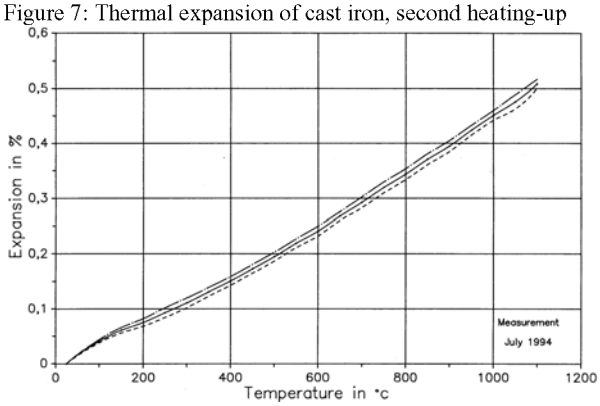

Figure 8: Thermal expansion of 3 different Alouette anode samples based on GLC coke

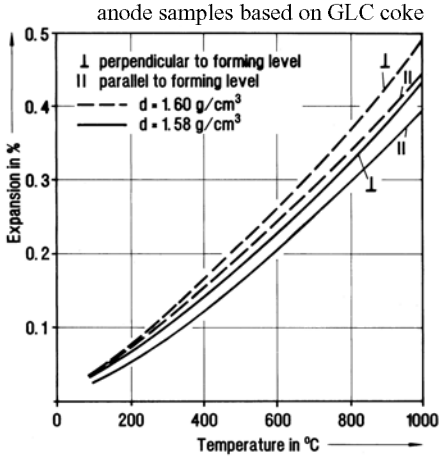

Figure 9: Thermal expansion of anode samples in the vertical and horizontal direction

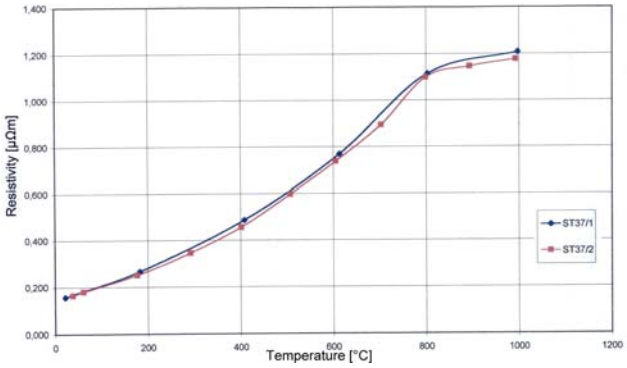

Figure 10: General electrical resistivity of mild steel

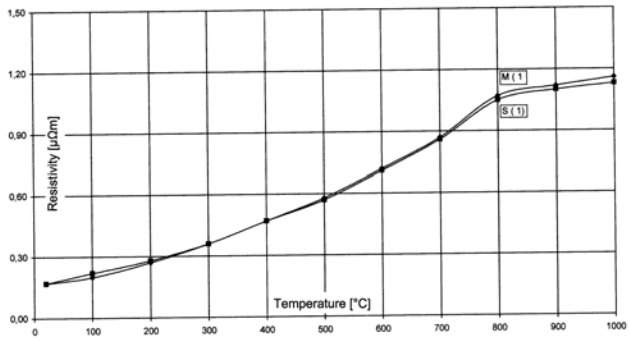

Figure 11: Electrical resistivity of Alouette stub steel

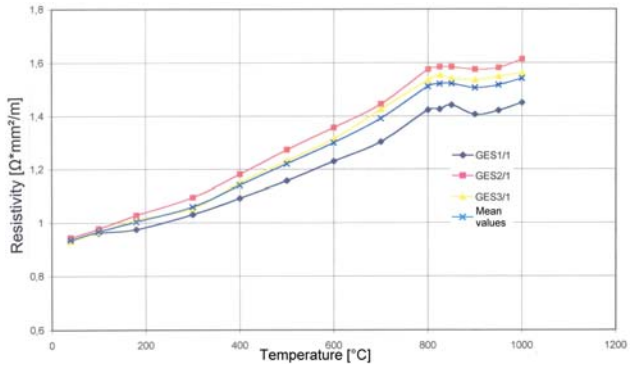

Figure 12: Electrical resistivity of 3 cast iron samples, first heating cycle

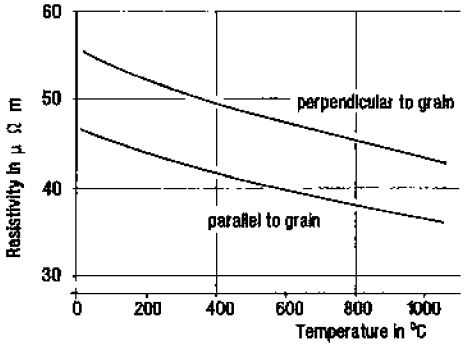

Figure 14: Electrical resistivity of an anode with butts

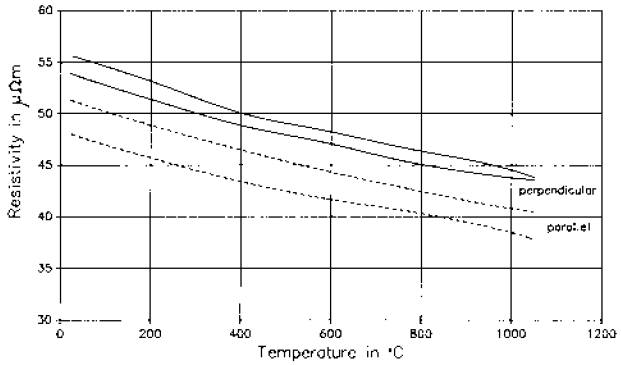

Figure 15: Electrical resistivity of 2 anode samples without butts

Thermal conductivity

The thermal conductivities of mild steel, cast steel, cast iron and anode carbon were measured by us as a function of temperature, and are graphically shown in Figures 16 to 19. Heat is withdrawn by the steel stub from the stub-anode region in the vertical direction. Therefore, temperature elevation appears in the pictures of thermal modeling near the stub insertion.

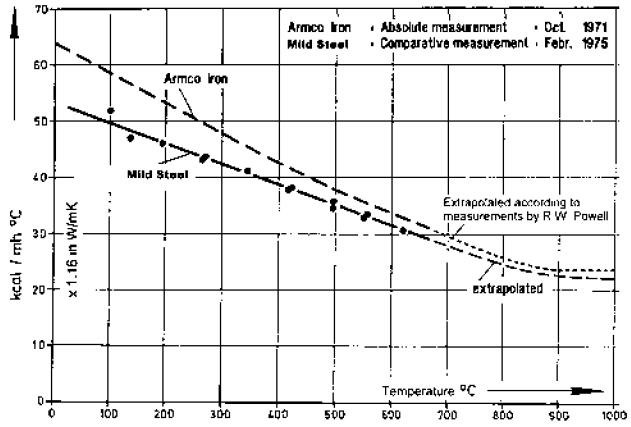

Figure 16:Thermal conductivity of mild steel

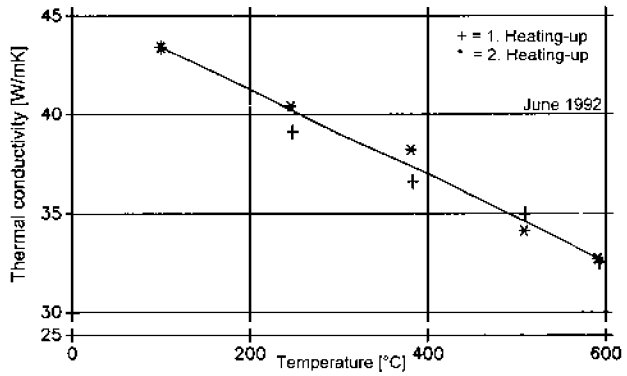

Figure 17: Thermal conductivity of cast steel GS38

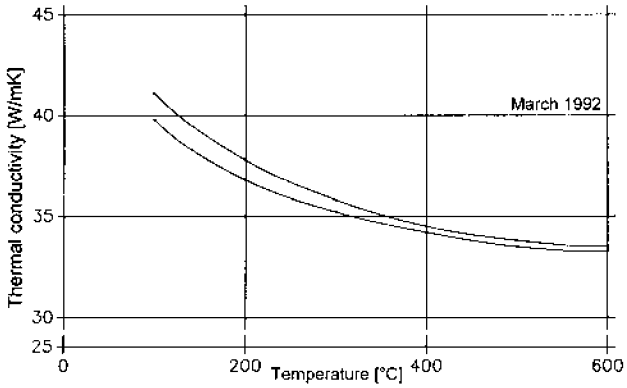

Figure 18: Thermal conductivity of cast iron (Example)

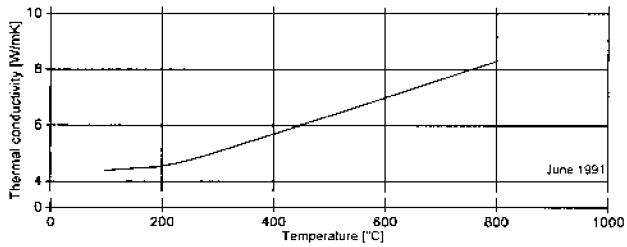

Figure 19: Thermal conductivity of anode carbon (Example)

Other physical properties

Stub steel may undergo creep at the final temperatures of anode cycle time (see Figure 20). Three phenomena can be observed: The stubs become gradually longer, their diameters smaller, and their lower, compressed immersion ends deform to a slightly conical shape. The carbon anode keeps its strength up to the final operating temperatures.

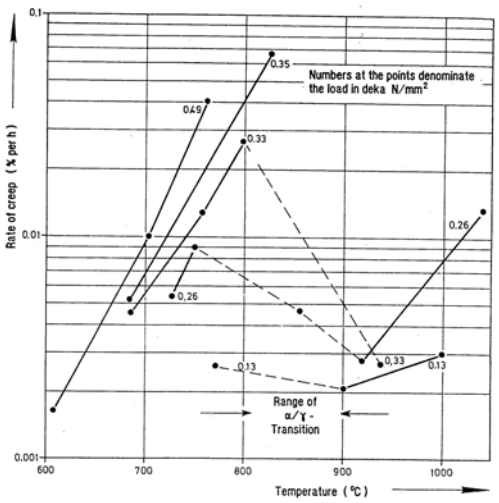

Figure 20: Creep of steel as a function of temperature and specific load

Composition of cast iron

Cast iron for anode rodding is a very special sector of application. The properties of cast iron were primarily developed and optimized for a great variety of foundry products, which are preferably used at ambient or relatively low temperatures. The main alloying elements of cast iron are carbon, silicon, phosphorus and manganese. Table I gives an indication of how these elements affect cast iron properties.

Table I: Effect of alloying elements on cast iron properties

	C	Si	P	Mn	S	Other
Melting point	++	+	++	o	++	+
Fluidity (Viscosity)	++	-	++	o	+	o
Wettability	o	-	+	o	+	o
Shrinkage (Liquid-solid transition)	+	++	-	o	o	o
Carbon solubility (Saturation)		- -	- -	+	o	o
Thermal expansion	-	+	o	o		
Growth by C precipitation	++	+	+			
(in the solid state at elevated temperatures)						
Strength		+	-	++	- -	+
Electrical resistivity	- -	- -	- -	-	-	-

Sulphur is considered to be an accompanying element with adverse effects on cast iron, particularly on strength and low-temperature softening. It is therefore eliminated from cast iron to levels below 0.05%. Cast iron picks up sulphur from the surrounding anode carbon during each anode cycle. It may form FeS layers on the cast iron thimble, which lead to an increase of electrical resistance at the interface between cast iron and anode. This phenomenon could be demonstrated by a scanning microprobe investigation (see Figures 21 – 23). Two metallographic pieces were cut from the thimble, one from the upper wall (Sample 1M) and another one from the bottom part (Sample 1B). The count intensities of sulphur (Red line, denoted by S) and carbon (Green line, denoted by C) were scanned across the wall thickness. A high sulphur peak can be noticed at the outside surface of the upper thimble wall (see Figure 22). The sample 1B from the thimble bottom, which was partially open, indicates a lot of sulphur pick-up at the outside as well as at the inside surface.
This result gives rise to the assumption that sulphur does not only bind with iron by solid diffusion but more likely by reaction with a sulphur-containing gas phase, for example, COS.

Several desulphurization methods are known. We prefer for this purpose calcium carbide, because it serves simultaneously as a carburizing agent. Manganese added as ferromanganese captures residual sulphur as MnS, but it seems to be expensive using ferromanganese for complete desulphurization.

Carbon and silicon are the predominant elements in cast iron. It is generally assumed that iron is saturated with carbon at the eutectic point at 1150°C and 4.3% C, but hypereutectic concentrations are possible. Alloying elements, especially silicon, interfere with carbon saturation by partial displacement of carbon according to the corresponding phase diagrams. Carbon saturation is described by the formula:

$$S_C = \%\ C / (4.23 - 0.312\ Si - 0.33\ P + 0.066\ Mn)\ \% \qquad (1)$$

If phosphorus is missing, a simplified formula for the carbon equivalent CE is used:

$$CE = \%\ C + 0.33\%\ Si = 4.3 \qquad (2)$$

Carbon makes cast iron more fluid than silicon. It has already been mentioned that in rapidly cooled cast iron (white cast iron) carbon is present as cementite, Fe_3C, and is precipitated from cementite as graphite, when the thimbles are heat-treated in the anode above 700°C. With regard to the carbon and silicon concentration in cast iron, quite different specifications are encountered. According to our stub-anode voltage drop measurements it is favorable to target a high carbon content in the range of 3.4 – 3.6% and a reduced silicon content of about 2.5%. The most important effect of silicon is its volume expansion on solidification, which causes a lower shrinkage of cast iron from the liquid to the solid state. Silicon is commonly added to cast iron as ferrosilicon. Silicon carbide can be used instead of FeSi. This alloying method allows to also introduce carbon to the melt.

The pronounced advantage of phosphorus in cast iron is its pronounced effect on cast iron fluidity. The contact between cast iron and anode carbon is enhanced by phosphorus and a lower stub-anode voltage drop has been observed. The big disadvantage of phosphorus is the fact that it may enter the molten electrolyte by attack of the cast-iron thimbles. The detrimental effects of phosphorus in electrolysis are contaminant of primary aluminium, lower current efficiency and substantial recirculation by dry scrubbing. A study on the sources of phosphorus in aluminium reduction cells at Alouette and other smelters proved that about 50% of the intake of phosphorus to the electrolytic bath stemmed from corroded thimbles. For this reason, phosphorus has been excluded from many types of cast iron to a minimum <0.1%. According to own measurements phosphorus increases the electrical resistivity and reduces the thermal conductivity of cast iron significantly.

In foundry cast iron manganese has the clear function to render strength. Although manganese is usually present in cast iron for anode rodding in the range of 0.6 – 0.8%, it is believed that rodding cast iron will be still strong enough with less manganese.

Figure 21: Samples taken from a cast iron thimble for microprobe investigation

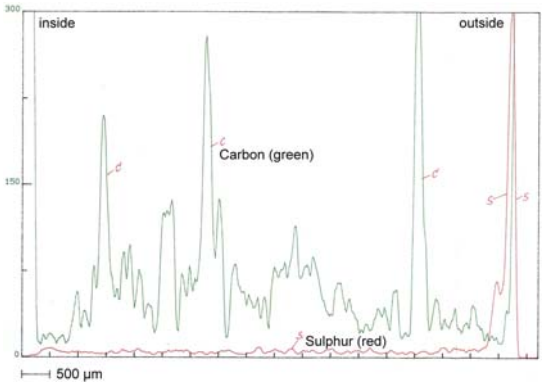

Figure 22: Counting intensity of sulphur and carbon across the upper thimble wall

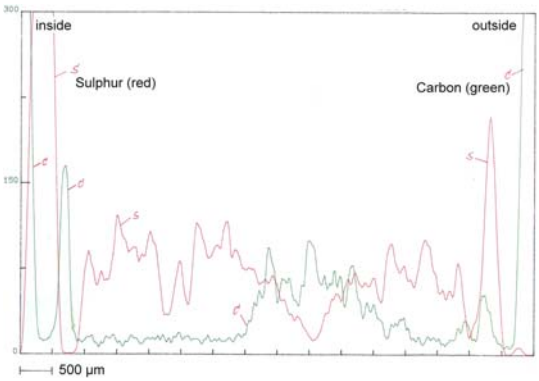

Figure 23: Counting intensity of sulphur and carbon across the bottom part of the thimble

Measurement of the stub-anode voltage drop in operational cells

Very often the task is set to establish a voltage balance for representative reduction cells in the potline, where voltage drops are measured step by step at defined reference points from the entry to the exit of current. Along this line the potential of the stub-anode connection constitutes an integral part and is usually measured at halfway stage of the anode cycle time. If more precise voltage drop measurements are wanted over the total cycle time of an anode in the pot, special reliable contact means must be prepared beforehand.

The method of voltage drop measurement on the AP30 cells at Alouette was as follows: 10 mm thick nickel rods with tapered ends were rammed into drilled holes and isolated by sillimanite tubes against the anode and cover material. Two rods were inserted at each stub of the hexapod, one in the cast iron thimble, the other one in the anode. Thus, six readings of potential were taken on one anode assembly. The mean value of the six voltage drop measurements was referred to the current flow in the anode stem. The amperage in the anode stem was measured by means of a Halmar tong-test instrument. Examples of measuring results at Alouette with the existing stubhole design are given in Figures 24 to 29. A typical example of voltage drop measurement between stub and anode is given in Figures 24 and 25 for the initial period of 20 h after anode changing and for the subsequent period up to 96 hours. The temperature change over this period of time is shown in Figure 26. More detailed measuring results of voltage drop are represented in the three diagrams Figures 27 – 29 for the individual steps of thimble-anode, stub-thimble and the total of both, namely stub-anode. It is seen from the diagrams in Figures 28 and 29 that the average voltage drop over approximately 90% of the anode rota time is about 12 mV between stub and thimble and about 120 mV between stub and anode. A relatively large voltage drop variation of the individual stubs can be noticed. In a number of other measuring series the individual values were closer together.

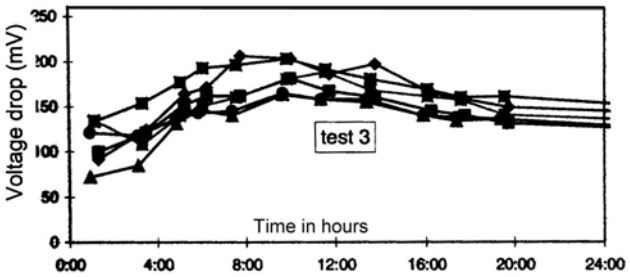

Figure 24: Voltage drop stub-anode for the first 20 hours

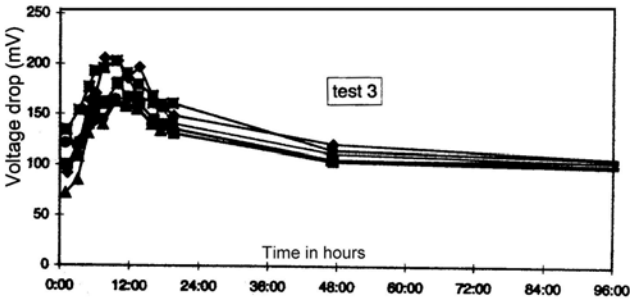

Figure 25: Voltage drop stub-anode for the first 4 days

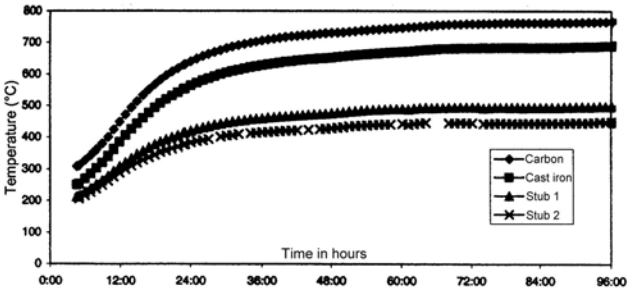

Figure 26: Evolution of temperatures after anode changing for the first 4 days

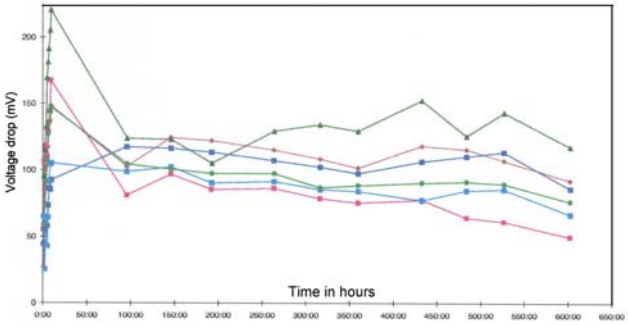

Figure 27: Voltage drop between cast iron and anode

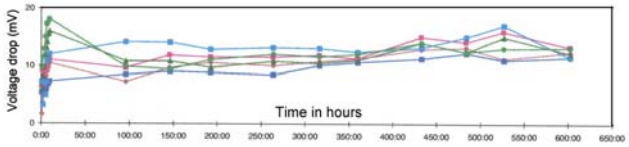

Figure 28: Voltage drop between stub and cast iron

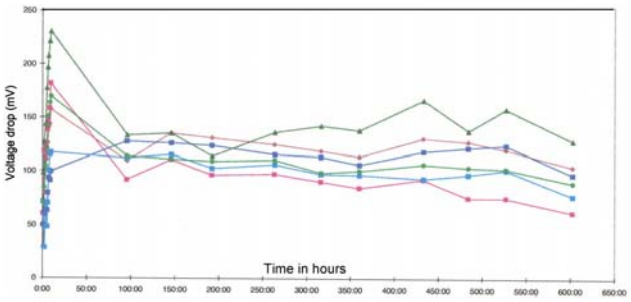

Figure 29: Voltage drop between stub and anode

Attempts were made to improve the voltage drop of the stub-anode connection by modification of the stubhole shape and profile. In Figure 30 the mean voltage drop of these tests is plotted versus the wall contact area. It is surprising that the larger contact area resulted in a higher voltage drop. It has been concluded from these results, that it is not the contact surface but the contact pressure, which determines the voltage drop cast iron – anode. An annular groove in the bottom of the stubhole improved the voltage drop significantly at the beginning of the anode cycle time.

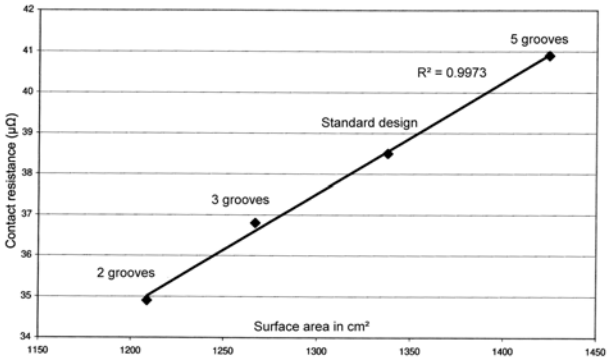

Figure 30: Contact resistance cast iron – anode versus wall contact area of modified stubholes

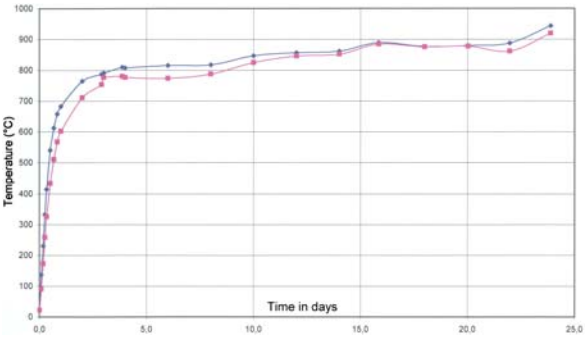

Figure 31: Temperature at inside and outside stubs versus anode cycle time

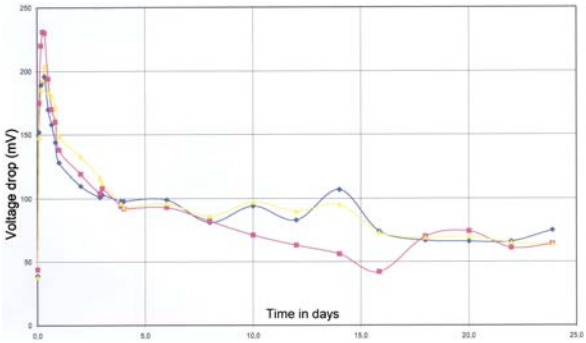

Figure 32: Voltage drop at 3 stubs versus anode cycle time

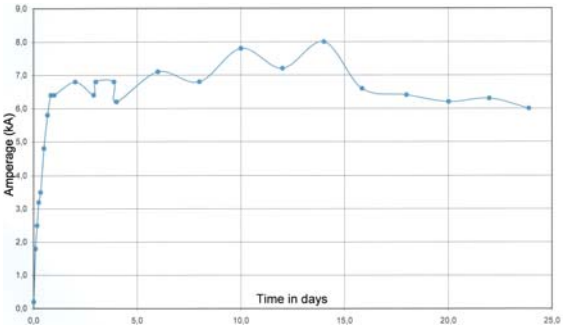

Figure 33: Amperage per anode versus anode cycle time

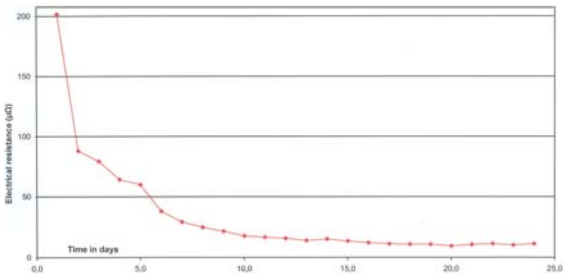

Figure 34: Electrical resistance versus anode cycle Time

Bench-scale measurements of contact resistances

The experimental set-up for the resistance measurements in the laboratory is shown in Figure 36. The measuring program comprised round steel bars of 70, 80, 90, 100 and 110 mm. The width of the annular gaps between the cylindrical steel bars and the machined cylindrical stubholes in the graphite blocks, which were filled with cast iron, varied from 7 to 17 mm. The 70 mm steel core was, for instance, rodded with cast iron sleeves of 7, 9, 11 and 13 mm in thickness, the 110 mm steel bar with 9, 11, 13 and 16 mm thick cast iron sleeves. The casting conditions and the composition of cast iron were kept constant for all the rodding tests. The bottom part of the round steel bars was isolated against the graphite block.

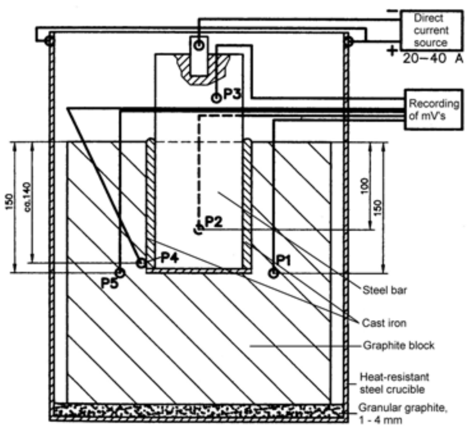

Figure 36: Experimental arrangement for ER measurements between round steel bar and graphite block

The following results were found in these rodding experiments with subsequent resistance measurements on heating-up:

- In the lower temperature range up to about 600°C, the contact resistances increase with thickness of the cast iron sleeves due to the higher shrinkage of the thicker cast iron layers. Above 600°C the differences in the electrical resistance (ER) disappear (see Figure 37).
- The contraction of steel and cast iron at the α to γ phase transition becomes visible as a slightly higher contact resistance (see Figure 38).
- Above 700°C the total expansion of steel and cast iron is decisive for the final contact resistance (see Figures 39 and 40).

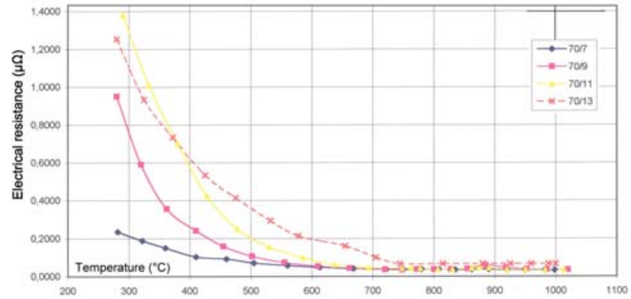

Figure 37: Effect of cast iron shrinkage on the ER between steel bar and graphite block as a function of temperature

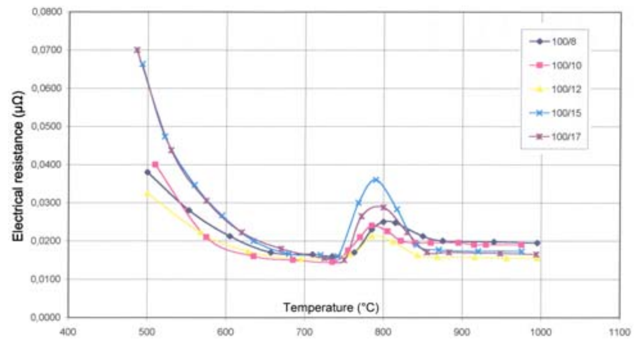

Figure 38: Effect of steel and cast iron shrinkage in the range of α-γ phase transition on the Electrical resistivity

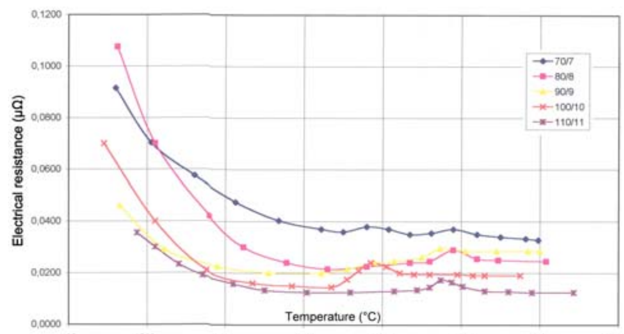

Figure 39: Electrical resistivity between steel and graphite as a function of temperature and of the combined effect of steel bar diameter and thickness of cast iron sleeve

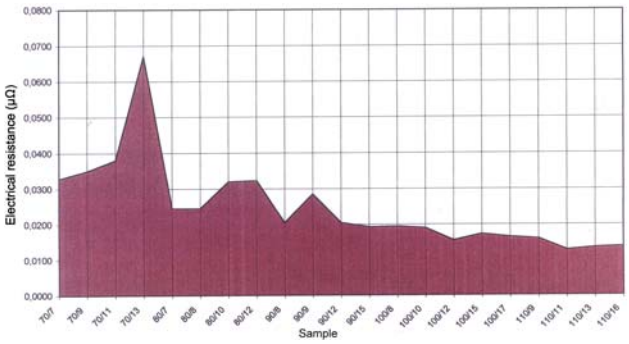

Figure 40: Electrical contact resistance at 1000°C between steel and graphite as a function of steel bar diameter and thickness of cast iron sleeve

Conclusions

- There is still a margin for the improvement of the stub-anode voltage drop by design measurements.
- A high contact temperature above 700°C of the stub-anode connection should be attained as fast as possible.
- Consistent conditions of rodding as well as of anode temperature and current help minimizing the stub-anode voltage drop.
- Cast iron with a high carbon content and reduced silicon and phosphorus content is considered to be favorable.